

## TURBULENCE SCALINGS IN SUPERSONIC CHANNEL FLOW

Rainer Friedrich<sup>\*</sup>, Holger Foysi<sup>\*</sup>, Sutanu Sarkar<sup>\*\*</sup>

<sup>\*</sup>TU München, Fachgebiet Strömungsmechanik, D-85748 Garching, Germany

<sup>\*\*</sup>UCSD, Mechanical & Aerospace Engineering, La Jolla, CA 92093-0411, U.S.A.

**Summary** Direct numerical simulations of compressible channel flow have been performed at subsonic and supersonic Mach numbers with the aim to better understand effects of compressibility. The ability of outer and inner scalings to collapse profiles of turbulence stresses on to their incompressible counterparts is investigated. It turns out that such collapse is possible with outer scaling when sufficiently far from the wall, but not with inner scaling. Compressibility effects on the turbulent stresses, their anisotropy and their balance equations are identified. A reduction in the near-wall pressure-strain, is explained using a Green's function-based analysis of the pressure field.

### INTRODUCTION

Supersonic channel flow is a prototypical example of a high-speed internal flow that allows for a systematic study of compressibility effects in wall-bounded turbulence. Pioneering investigations of this flow have been made by Coleman et al. [1] and Huang et al. [2]. Coleman et al. [1] performed DNS of supersonic channel flow between cold isothermal walls with Mach numbers up to  $M = 3$ . They found that Morkovin's hypothesis, "the flow dynamics follows an incompressible pattern", holds for the most part, and that the Van-Driest log-law is valid. Huang et al. [2] observed that the turbulent stresses,  $\bar{\rho} R_{ij}$ , scale with the wall shear stress,  $\tau_w$ , and that semi-local scaling is useful. Lechner et al. [3], in their study of  $M = 1.5$  channel flow, reported that the anisotropy of the Reynolds stresses was changed relative to the corresponding incompressible values, but they did not provide any explanation. Morinishi et al. [4] simulated supersonic channel flow at  $M = 1.5$  with one wall isothermal and the other wall adiabatic, and found significant differences between the flows in the two halves of the channel. Based on this literature survey it appears that there are open issues regarding the behaviour of the turbulent stresses. The first objective of the current work is to evaluate the applicability of the incompressible fluctuating velocity scale (the friction velocity) and the inner and outer length scales to compressible flow where the density and viscosity are functions of position, and the second objective is to provide an explanation for the systematic change of the turbulent stresses with increasing Mach number.

### DETAILS OF DNS

The compressible Navier-Stokes equations are numerically solved using a pressure-velocity-entropy formulation following the algorithm of Sesterhenn [5]. The mean pressure gradient that drives the channel flow is replaced by a uniform body force. Both channel walls are cooled and kept at a temperature of  $T_w = 500$  K. Periodic boundary conditions are applied in stream- and spanwise directions. The compact 5<sup>th</sup>-order upwind scheme of Adams & Shariff [6] is used to discretize the Euler terms, the compact 6<sup>th</sup>-order scheme of Lele [7] for the molecular terms, and a 3<sup>rd</sup>-order low-storage Runge-Kutta scheme for the time advancement.

The numerical algorithm has been validated in [3] for a  $M = 1.5$  case and excellent agreement with data of [1] has been found. In the present work the mean mass flow rate is systematically increased so that the Mach number  $M = u_{av} / c_w$  based on the Reynolds cross-sectionally averaged velocity and the sound speed at wall temperature takes values between 0.3 and 3.0. The bulk Reynolds number  $Re = \rho_m u_{av} h / \mu_w$  is based on the cross-sectionally averaged mean density. It increases with  $M$ . The friction Reynolds number  $Re_\tau = \rho_w u_\tau h / \mu_w$ , with  $u_\tau = (\tau_w / \rho_w)^{1/2}$ , is a result of the simulation. Table 1 summarizes the flow parameters, computational box sizes and number of grid points used in the different compressible cases M0.3 to M3.0. Equidistant grids are taken in streamwise  $x_1$ - and spanwise  $x_3$ -directions. In the wall-normal  $x_2$ -direction, points are clustered using tanh-functions [3]. The compressible flow results are compared with the incompressible data of Moser et al. [8] at various Reynolds numbers:  $Re_\tau = 180, 395, \text{ and } 590$ , denoted by cases I1, I2, I3, respectively.

Case	M	Re	$Re_\tau$	$L_{x1}/h$	$L_{x2}/h$	$L_{x3}/h$	$N_{x1}$	$N_{x2}$	$N_{x3}$	$\Delta x_1^+$	$\Delta x_2^+_{min}$	$\Delta x_2^+_{max}$	$\Delta x_3^+$
M0.3	0.3	2820	181	9.6	2	6	192	129	160	9.12	1.02	4.21	6.84
M1.5	1.5	3000	221	$4\pi$	2	$4\pi/3$	192	151	128	14.46	0.84	5.02	7.23
M2.5	2.5	5000	455	$2\pi$	2	$2\pi/3$	256	201	128	11.16	1.17	7.46	7.44
M3.0	3.0	6000	560	$2\pi$	2	$2\pi/3$	256	221	128	13.37	0.89	9.38	8.91

TABLE 1. Flow and computational parameters

The flow physics in compressible channel flow with isothermal cold walls is different from that in incompressible channel flow mainly because of the large change in fluid properties. The mean temperature increases in the core of the channel due to viscous heating and, since  $\mu \sim T^{0.7}$ , so does the mean viscosity. The mean density, being inversely proportional to the mean temperature, decreases from its wall value with increasing  $x_2$ .

**PRESSURE-STRAIN CORRELATION**

The pressure-strain correlation,  $\Pi_{ij}$ , plays a key role in changing the turbulent stresses and associated anisotropy. It is observed that the pressure-strain profiles for all incompressible and compressible cases collapse in the outer region,  $x_2/h > 0.35$  when scaled with  $\tau_w u_{av} / h$  (outer scaling). In the inner region,  $\Pi_{ij}$  is reduced in compressible channel flow as compared to the incompressible counterpart. In an attempt to explain the underlying mechanism, an equation for the pressure fluctuations is derived taking the divergence of the momentum equation, and using mass conservation. After some algebraic manipulation, the following equation results for channel flow:

$$\nabla^2 p' = A_1 + A_2 + A_3 + B_1 + B_2 + C_1 + C_2 + C_3, \tag{1}$$

with

$$A_1 = -\bar{\rho} (u_i'' u_j'' - \overline{u_i'' u_j''})_{,ij}; \quad A_2 = -2 \bar{\rho} \bar{u}_{1,2} u_{2,1}''; \quad A_3 = \sigma'_{ij,ij}; \quad B_1 = -2 \bar{\rho}_{,2} (u_2'' u_j'' - \overline{u_2'' u_j''})_{,j}. \tag{2}$$

In incompressible flow, the terms  $A_1$  to  $A_2$  describe effects by nonlinear fluctuations and mean shear, respectively. In compressible flow, the additional terms involve effects by viscosity ( $A_3$ ), mean density gradients ( $B_1, B_2$ ) and by density fluctuations ( $C_1, C_2, C_3$ ). Neglecting the density fluctuations, eq. (1) can be interpreted as a Poisson equation for the pressure which accounts solely for mean density variations. In this case the rhs of (1) is replaced by  $\bar{\rho} f'$  and a Green's function analysis is performed. It turns out that the Green's function  $G$  is the same as that given by Kim [9] for incompressible channel flow. An extra inhomogeneous fluctuating term  $B'$ , however, appears in compressible flow due to nonzero wall-normal pressure gradient fluctuations. The pressure-strain correlation can finally be expressed in the form

$$\Pi_{ij}(x_2) = \int_{-1}^1 \bar{\rho}(x'_2) (G * f'(x_1, x_2, x_3, x'_2) s'_{ij}) dx'_2 + (B' s'_{ij}) \tag{3}$$

Fig. 1 shows a comparison of the analytical solution, eq. (3), and the DNS data for cases M0.3 and M1.5. The overall agreement is very good, confirming our ansatz that a variable-density extension of the Poisson equation is sufficient for obtaining the pressure-strain term in wall-bounded flows.

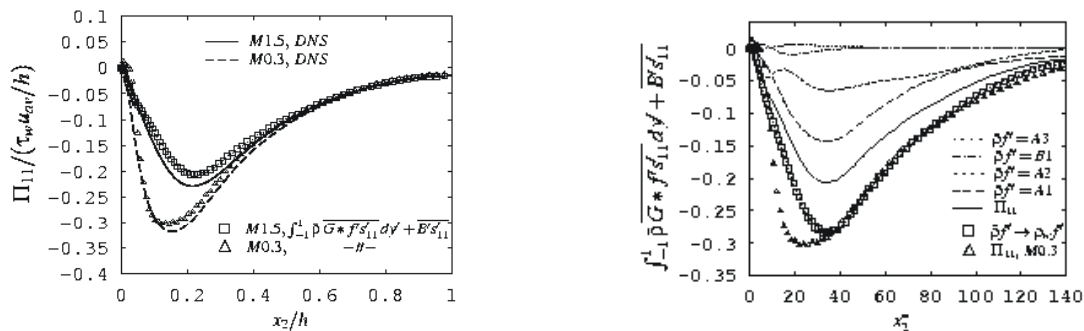


Figure 1. Left: Comparison of the DNS data with results using eq. (3) for the pressure-strain correlation. Right: Contribution of source terms,  $A_1$ -  $A_3$ ,  $B_1$  to eq. (3) in the case of  $\Pi_{11}$  are shown by lines for case M1.5.

**CONCLUSIONS**

Conventional outer scaling of the turbulent stresses with  $\tau_w$  collapses all compressible and incompressible profiles for  $x_2/h > 0.35$ . Similarly,  $\tau_w u_{av} / h$  is the proper outer scale for the pressure-strain correlation,  $\Pi_{ij}$ . The significant difference of compressible and incompressible turbulent stresses in the near-wall region is linked to a reduction in the pressure-strain correlation. A variable-density ansatz, neglecting wave-propagation in the pressure equation, leads to a simplified Green's function solution which identifies the reduction of  $\bar{\rho}$  with respect to its wall value as the primary reason for the observed decrease in  $\Pi_{ij}$ .

**References**

- [1] Coleman G., Kim J., Moser R.: Turbulent Supersonic Isothermal-Wall Channel Flow. *J. Fluid Mech* **305**:159-183, 1995.
- [2] Huang P., Coleman G., Bradshaw P.: Compressible Turbulent Channel Flows: DNS Results and Modeling. *J. Fluid Mech* **305**:185-218, 1995.
- [3] Lechner R., Sesterhenn, J., Friedrich, R.: Turbulent Supersonic Channel Flow. *J. Turbulence* **2**:1-25, 2001.
- [4] Morinishi Y., Tamano S., Nakabayashi K.: A DNS Algorithm Using B-Spline Collocation Method for Compressible Turbulent Channel Flow. *Comput. Fluids* **32**:751-776, 2003.
- [5] Sesterhenn J.: A Characteristic-Type Formulation of the Navier-Stokes Equations for High Order Upwind Schemes. *Comput. Fluids* **30**:37, 2001.
- [6] Adams N.A., Shariff K.: A High-Resolution Hybrid Compact-ENO Scheme for Shock-Turbulence Interaction Problems. *J. Comp. Phys.* **127**: 27, 1996.
- [7] Lele S.K.: Compact Finite Difference Schemes with Spectral-Like Resolution. *J. Comp. Phys.* **103**: 16-42, 1992.
- [8] Moser R., Kim J., Mansour N.N.: Direct Numerical Simulation of Turbulent Channel Flow up to  $Re_\tau = 590$ . *Phys. Fluids* **9**: 943-945, 1999.
- [9] Kim J.: On the Structure of Pressure Fluctuations in Simulated Turbulent Channel Flow. *J. Fluid Mech* **205**:421-451, 1989.